Journal Pre-proof

A shield of defense: Developing ballistic composite panels with effective electromagnetic interference shielding absorption

Nisrin Rizek Abdelal

PII: S2214-9147(23)00232-5

DOI: https://doi.org/10.1016/j.dt.2023.08.018

Reference: DT 1319

To appear in: *Defence Technology*

Received Date: 21 June 2023

Revised Date: 17 August 2023

Accepted Date: 29 August 2023

Please cite this article as: Abdelal NR, A shield of defense: Developing ballistic composite panels with effective electromagnetic interference shielding absorption, *Defence Technology* (2023), doi: https://doi.org/10.1016/j.dt.2023.08.018.

A shield of defense: developing ballistic composite panels with effective electromagnetic interference shielding absorption.

Nisrin Rizek Abdelal*

Mechanical engineering, Jordan University of Science and Technology, Irbid 22110, Jordan

*Corresponding author: Email: nrabdelal@just.edu.jo

A shield of defense: developing ballistic composite panels with effective electromagnetic interference shielding absorption.

Abstract

The primary goal of this study is to develop cost-effective shield materials that offer effective protection against high-velocity ballistic impact and electromagnetic interference (EMI) shielding through absorption. Six fiber-reinforced epoxy composite panels, each with a different fabric material and stacking sequence, have been fabricated using a hand-layup vacuum bagging process. Two panels made of Kevlar and glass fibers, referred to as (K-NIJ) and (G-NIJ), have been tested according to the National Institute of Justice ballistic resistance protective materials test NIJ 0108.01 Standard-Level IIIA (9 mm × 19 mm FMJ 124 g) test. Three panels, namely, a hybrid of Kevlar and glass (H-S), glass with ceramic particles (C-S), and glass with recycled rubber (R-S) have been impacted by the bullet at the center, while the fourth panel made of glass fiber (G-S) has been impacted at the side. EMI shielding properties have been measured in the X-band frequency range via the reflection-transmission method. Results indicate that four panels (K-NIJ, G-NIJ, H-S, and G-S) are capable of withstanding high-velocity impact by stopping the bullet from penetrating through the panels while maintaining their structural integrity. However, under such conditions, these panels may experience localized delamination with variable severity. The EMI measurements reveal that the highest absorptivity observed is 88% for the K-NIJ panel at 10.8 GHz, while all panels maintain an average absorptivity above 65%. All panels act as a lossy medium with a peak absorptivity at different frequencies, with K-NIJ and H-S demonstrating the highest absorptivity. In summary, the study results in the development of a novel, cost-effective, multifunctional glass fiber epoxy composite that combines ballistic and electromagnetic interference shielding properties. The material has been developed using a simple manufacturing method and exhibits remarkable ballistic protection that outperforms Kevlar in terms of shielding efficiency; no bullet penetration or back face signature is observed, and it also demonstrates high EMI shielding absorption. Overall, the materials developed show great promise for various applications, including the military and defense.

Keywords: Ballistic; FRP composite; EMI shielding; Absorptivity; CT-scan; NIJ test; Bullet; Defense

1. Introduction

The evolution of protective equipment designed to safeguard human bodies against enemy attacks has a historical origin that dates to ancient civilizations, where materials such as animal skin, wood, stone, and steel were first utilized. The demand for lightweight and high-performance armor materials has been increasing in recent years, especially in the defense and law enforcement sectors, due to the increase in international and civilian conflicts [1−4]. Ballistic composite materials, composed of fiber-reinforced polymeric matrices, are now considered one of the most promising solutions as they provide high-performance protection against high-velocity impacts. They offer a combination of mechanical strength, low weight, and improved energy absorption and dissipation through a combination of mechanisms such as fiber breaking and matrix cracking [5−8]. Multilayered high-performance fabrics and hard armors reinforced with metal, ceramics, or polymer plates exhibit high specific strength and stiffness and can be tailored to meet the specific requirements of various applications. The ballistic behavior of composites is influenced by factors such as microstructure, fiber orientation, matrix properties, number of fabric layers, and fiber-to-matrix weight fraction. Numerous research studies have been conducted to investigate the ballistic behavior of composites and gain a deeper understanding of their underlying mechanisms [9−11]. Among the various types of composite materials, those made of ultra-high molecular weight polyethylene (UHMWPE) fibers and Kevlar fabrics have been proven to be highly efficient in resisting high-velocity impacts. For example, Grujicic et al. presented a new model for ballistic materials made of cross-plied (UHMWPE) fiber and polymeric-matrix composite laminates [12]. The model was constructed using fiber-polymer material properties, unit-cell microstructural characteristics, and unit-cell level finite element analysis. The model was validated through simulations of the non-linear dynamic behavior of the armored laminates using two types of bullets and projectiles. The simulation results were compared with the experimental data and showed good agreement in different aspects, such as the effectiveness of the armor panels with varying densities in stopping bullets at different initial speeds, the spatial distribution of damage inside the panels, and the presence of three stages in the armor penetration process. Weerasinghe et al. conducted an experimental and numerical study to investigate the influence of the matrix rigidity of four different matrix materials on the impact behavior of (UHMWPE) textile composites [13]. The composite laminates were prepared using plain-weave Spectra fibers, and their behavior under high-velocity impact was evaluated by striking the laminates with spherical steel projectiles from a gas gun. The experimental results indicated a gradual change in the mode of deformation of textile composites, transitioning from membrane stretching to plate bending with increasing matrix rigidity and thickness. The flexible matrix composites (composites with lower matrix rigidity and membrane stretching mode) exhibited higher impact resistance and energy absorption capacity and displayed higher resistance to perforation compared to their rigid matrix counterparts. The numerical model results demonstrated that the development of stress and strain in the composites with a more rigid matrix was concentrated in the vicinity of the impact sites, resulting in greater local deformation and reduced perforation resistance. Stopforth et al. aimed to design a safe bullet-proof vest using a gel/Kevlar composite by varying the Kevlar′s weight and number of layers [14]. To achieve this goal, several ballistic experiments using 9 mm Parabellum ammunition were conducted on various combinations of ballistic gel and Kevlar layers of varying weights. Results provided valuable insight into the number of layers and areal density represented by grams per square meter (GSM), required to halt the 9 mm bullet from penetrating the composite. At least twenty-one layers of the 200 GSM Kevlar were considered effective to stop the 9 mm Parabellum bullet, which is one of the most widely used types of ammunition worldwide. In another attempt to study the effectiveness of natural fiber composites in resisting high energy ammunition, Filho et al. evaluated the effectiveness of piassava natural fibers-reinforced epoxy composites prepared using press molding against high energy ammunition [15]. The effect of fiber volume fraction on ballistic performance was studied through macro and microscopic analysis of the failure modes. The results obtained were assessed using statistical analysis. It was concluded that composites reinforced with a 50% fiber volume fraction demonstrated the best energy absorption performance of about 205 joules, which was comparable to that of Kevlar.

Ballistic composites can be tailored to fulfill specific performance requirements while maintaining their resistance to impact, thus transforming them into multifunctional composites [16−18]. For example, in the aerospace industry and military applications, it is often necessary to have lightweight structural members, equipment boxes, or even large containers that possess high impact resistance, while also providing electromagnetic interference (EMI) shielding for protecting the electronic payload from mechanical shock and interference of communication signals [19, 20]. Interference from electromagnetic (EM) waves can lead to malfunctioning of nearby electronic devices, disturbing signals, and potentially affecting human health. To mitigate these harmful effects, the utilization of shielding materials is necessary to protect nearby electronic devices, communication systems, and individuals from the potential dangers of electromagnetic waves [21−24]. Numerous research studies have explored the EMI shielding properties of composite and nanocomposite materials for various applications [25−31]. However, limited attention has been given to the development of composites that combine both ballistic and EMI shielding characteristics. One notable exception is the work by Micheli et al., where they investigated the ballistic and EMI shielding behavior of a multifunctional hybrid laminated composite material specifically designed for aerospace applications [32]. They prepared hybrid composite laminates consisting of layers of Kevlar fabrics and carbon fiber (CF)-reinforced epoxy matrix incorporating (CNT) fillers. The laminates consisted of six layers of carbon and two layers of Kevlar in the following stacking sequence: three CF layers following the scheme (0°–90°), two layers of biaxial Kevlar fabric, and again three layers of CF ply as above with a laminate thickness of 3.5 mm. Two types of composite laminates were prepared based on the matrix, the first was with epoxy loaded with CNT, and the second was with neat epoxy. EMI shielding properties were tested in the 0.8–8 GHz frequency range, whereas energy absorbing capability was tested using metallic bullets fired at velocities of 400 m/s and 1000 m/s to simulate the low-energy mechanical shocks in aerospace structures. Results showed a maximum shielding effectiveness of 80 dB at 1 GHz and about 58 dB at around 8 GHz for both types of composites. This is because the dominant effect was associated with the presence of the carbon fibers, whereas the effect of incorporating CNTs in the epoxy matrix was small. Results also showed that both types of composites can absorb high impact energy of 600 joules at 400 m/s with local delamination of the layered structure.

Despite their widespread use, the ballistic behavior of composite laminates remains a complex issue that needs further investigation. Also, while previous research has focused on preparing ballistic materials or materials for electromagnetic interference shielding separately, the combination of these two has been very limited. Therefore, in this research, an experimental study is conducted to develop cost-effective multifunctional fiber-reinforced epoxy matrix composites that possess effective high-velocity ballistic properties and electromagnetic interference shielding via absorption. Six composite panels were fabricated using a hand-layup vacuum bagging process, each with a different fabric material and stacking sequence. Two panels, made of Kevlar and glass fibers (K-NIJ and G-NIJ), underwent the NIJ 0108.01 Standard- Level IIIA (9 mm × 19 mm FMJ 124 g) test. Three other panels, namely, a hybrid of Kevlar and glass (H-S), glass with ceramic particles (C-S), and glass with recycled rubber (R-S), were impacted by the bullet at the center, while the fourth panel made of glass fiber (G-S) was impacted at the side. The EMI shielding properties of the materials were characterized in the X-band frequency range using the reflection-transmission method. In conclusion, the developed, cost-effective composite materials that combine ballistic and EMI shielding properties show promise for various applications, including military and defense.

2. Methodology

2.1. Materials

In this study, two distinct types of reinforcing fibers, namely Kevlar fabrics and glass fibers, were utilized to manufacture the ballistic composite laminates. The Kevlar fabric obtained from DuPont Kevlar in the USA featured a plain weave double stitch with areal density of 475 g/m^2, a fabric width of 1.8 m, a yarn denier of 3000, and a fabric thickness of 0.8 mm. The fabric′s breaking strength was 280 kN/m in the length direction and 315 kN/m in the width direction. Three types of glass fibers were utilized, including randomly oriented (GR) glass fiber with areal density of 450 g/m^2 and a thickness of 0.6 mm obtained from the domestic market. The second type was Vectorply E-BX 1700 double bias ±45° stitched E-glass cloth with areal density of 615 g/m^2 and a thickness of 0.6 mm obtained from The Epoxy Experts, a Division of Polymer Composites Inc. Ontario, California, USA. The third type was Bruswick U-1301 unidirectional glass with areal density of 440 g/m^2 and a thickness of 0.6 mm, sourced from Fiber Glass Industries Inc., USA. The used epoxy resin matrix consists of two parts: part A, the diglycidyl ether of bisphenol A (DGEBA), and part B, the hardener (curing agent), cycloaliphatic amine, which were supplied by The Epoxy Experts-Polymer Composites Inc. Ontario, California, USA, with a density of 1.1 g/cm^3 and viscosity of 800–1,200 cPS at 25 °C when mixed. Silicon carbide particles with average particle size of 9–10.5 μm were used in this study. The study also incorporated recycled tire rubber as a component.

2.2. Panel fabrication

In this study, the hand-layup vacuum bagging process was used to fabricate the composite panels. Herein, a detailed, step-by-step description of this fabrication process is illustrated in Fig. 1.

To ensure the quality of the laminates, a glass plate that was used as the mold was thoroughly cleaned to eliminate any potential contaminations. Next, release agent was applied to the glass mold surface and covered with a non-porous Teflon (TFNP 234) sheet to facilitate the removal of the laminate after curing, as shown in Fig. 1(a). Then, the fabric was cut to the desired dimensions and weighed using a digital scale. The resulting weight was used to determine the weight ratio of fabric to matrix, which was targeted at approximately 60:40. Any potential losses were taken into account during this process. The two components of the epoxy matrix were mixed at a 2:1 weight ratio, and evenly distributed on the fabrics, layer by layer, using a squeegee as shown in Figs. 1(b) and 1(c). The impregnated fabrics were then covered successively by a Teflon sheet, an aluminum caul plate and a breather, as shown in Figs. 1(d) and 1(e). The setup was covered with a vacuum bag and tightly sealed with sealant tape before being connected to a vacuum pump, as illustrated in Fig. 1(f). The composite panel was left under vacuum for 20 hours at ambient temperature for curing and then placed in an oven at 70 °C for 3 hours for post-curing. To fabricate the panel containing silicon carbide particles, 10 wt% of SiC was added to the epoxy matrix and mixed thoroughly. The mixture was then sonicated using probe sonicator at an amplitude of 30 for 40 minutes to ensure proper dispersion of the particles. After sonication, the resulting SiC/epoxy mixture was vacuum degassed to remove any air bubbles. Once the degassing process was complete, the curing agent was added to the mixture, and finally, the mixture was evenly distributed onto the fabric layers using the aforementioned procedure.

Six composite laminates were fabricated using different materials and stacking sequences. Table 1 provides details of the panels utilized in the investigation, including their names and associated notations, as well as their specifications. Two panels were fabricated according to the NIJ test standard with dimensions of 31 cm × 31 cm, while four panels were fabricated with a smaller size of 20 cm × 20 cm to be fired at the center or at the side. The resulting panels were carefully designed to meet specific requirements and were subjected to a range of tests to evaluate their performance. The methods and results of these tests will be discussed in details in subsequent sections.

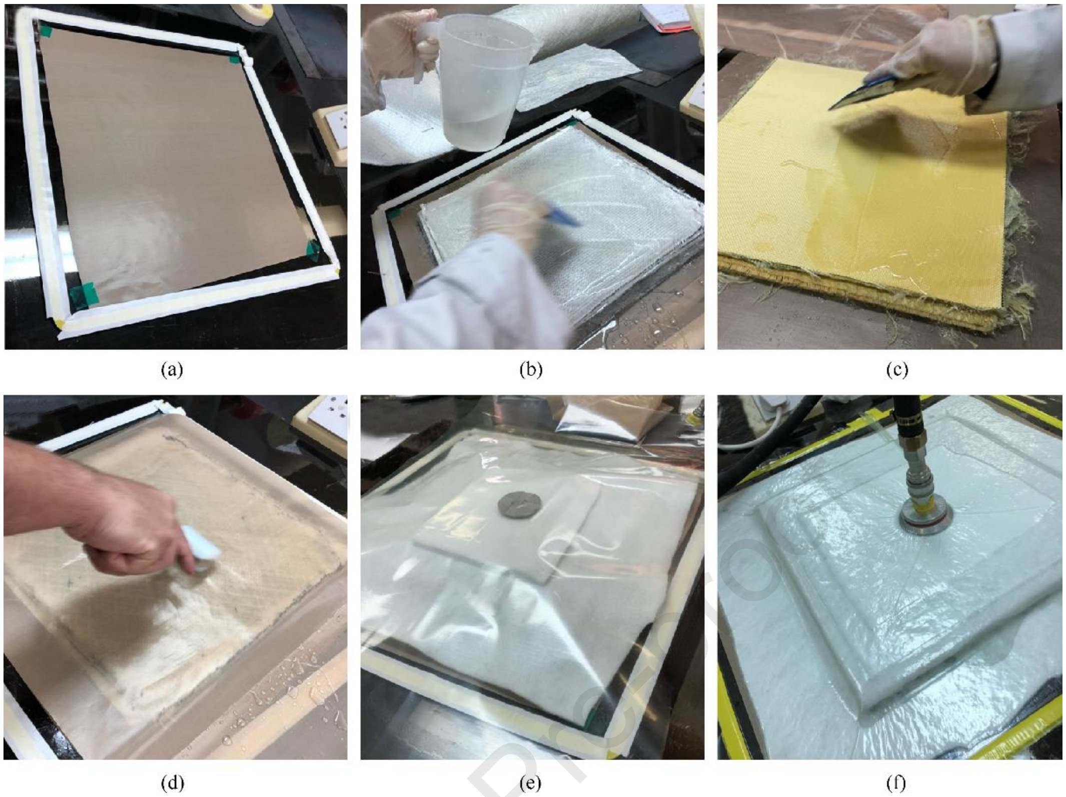

Fig. 1. Panel fabrication process: (a) TFNP 234 on glass mold; (b) and (c) Spreading the epoxy mixture on the glass and Kevlar fabrics; (d) Rolling the fabrics to remove the excess epoxy; (e) Breather and vacuum bag covering the composite; (f) Setup under vacuum.

Table 1

Details of the fabricated panels. GR means randomly oriented glass fiber, K means Kevlar, S means small size panel.

Panel name	Materials	Stacking sequence	Mass/g	Dimensions/(cm×cm×cm)
Kevlar (K-NIJ) NIJ test	Kevlar fabrics and epoxy	15 layers of Kevlar fabrics	1616.5	31×31×1.8
Glass (G-NIJ) NIJ test	Glass fiber and epoxy	26 layers $\pm45°_4/GR_8/\pm45°_2/GR_8/\pm45°_4$	2518.8	31×31×1.7
Hybrid (small) (H-S) Center shot	Glass fiber sandwiched between two faces of Kevlar fabrics in an epoxy matrix	20 layers $K_3/GR_{14}/K_3$	861.1	20×20×1.6
Ceramic (small) (C-S) Center shot	Glass fibers and Silicone carbide particles	18 layers $\pm45°_2/ GR_{14}/\pm45°_2$	860.2	20×20×1.5

	incorporated in the epoxy matrix			
Rubber (small) (R-S) Center shot	Glass fibers and recycled crushed tire rubber incorporated in the epoxy matrix	18 layers $\pm45°_2$/ GR_{14}/$\pm45°_2$	874.8	20×20×1.5
Glass (Small) (G-S) Side shot	Glass fiber in epoxy matrix	24 layers $\pm45°_2/0°/90°/\pm45°_2/0°/90°/GR_{12}/\pm45°_2/90°/0°$	986.2	20×20×1.6

2.3. Ballistic resistance testing

The National Institute of Justice (NIJ) ballistic resistance protective materials tests were conducted at the Test and Evaluation Department- Ballistic testing facility at Jordan Design and Development Bureau (JODDB) Company in Jordan. The NIJ ballistic resistance protective materials test at JODDB utilized the latest technology and equipment to accurately evaluate the panels and determine the results of the test. The test used was the NIJ 0108.01 Standard-Level IIIA (9 mm×19 mm FMJ 124 g) test protocol using the setup shown in Fig. 2.

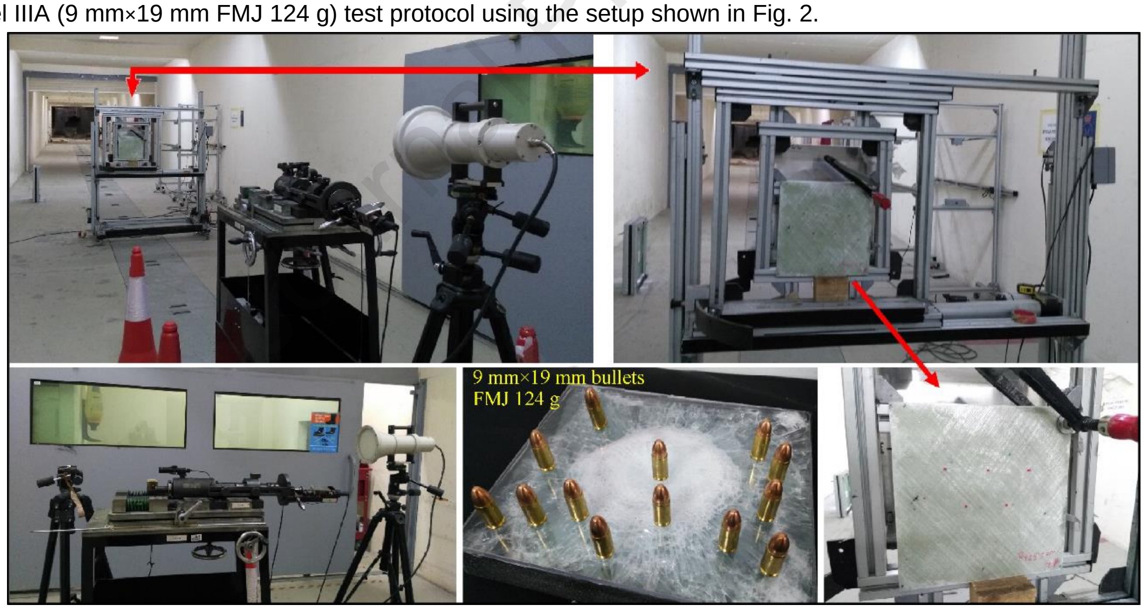

Fig. 2. Ballistic test setup. NATO universal Ballistic Breech with standard barrel 9 mm×19 mm: NIJ 0108.01 Standard-Level IIIA (9 mm×19 mm FMJ 124 g) test. Ruler, Doppler radar, distance laser.

The weapon used was the NATO Universal Ballistic Breech, which was equipped with a standard 9 mm×19 mm barrel for stability of the projectile. The bullet type was 9 mm×19 mm FMJ, with a total mass of 124 grams. The test panels were placed at 5 m from the gun, and they were shot from the NATO Universal Ballistic Breech with a muzzle velocity of 426±15 m/s. 426±15 m/s is the bullet velocity required by the NIJ standard test, which means the bullet velocity should be in the range (411–441 m/s) for the test to be reliable and certified. Fig. 3 shows that all bullet velocities fall within the specified range. The velocity measurements were taken using a Doppler radar system located 2.5 m from the muzzle with an uncertainty of ±0.4 m/s; which means if the measured velocity is 440 m/s, the actual velocity will be in the range of 439.6–440.4 m/s. Velocity was measured when the bullet was 2.5 m from the panel, although the panel was 5 mm away from the gun. The test equipment also included a ruler, digital caliper, temperature and humidity meter, and a distance laser measuring device. The test panels were supported by a fixture that allowed for easy adjustment of their position and angle, ensuring that it was perpendicular to the line of flight of the bullet at the point of impact. The aiming process was accomplished using standard laser bullets. Two panels, namely K-NIJ and G-NIJ, were tested according to the standard NIJ testing protocol; three panels, H-S, C-S, and R-S, were shot at the center, while G-S was shot at the side, as shown in Fig. 3. Fig. 3 details the bullet impact velocity and the impact pattern of each panel.

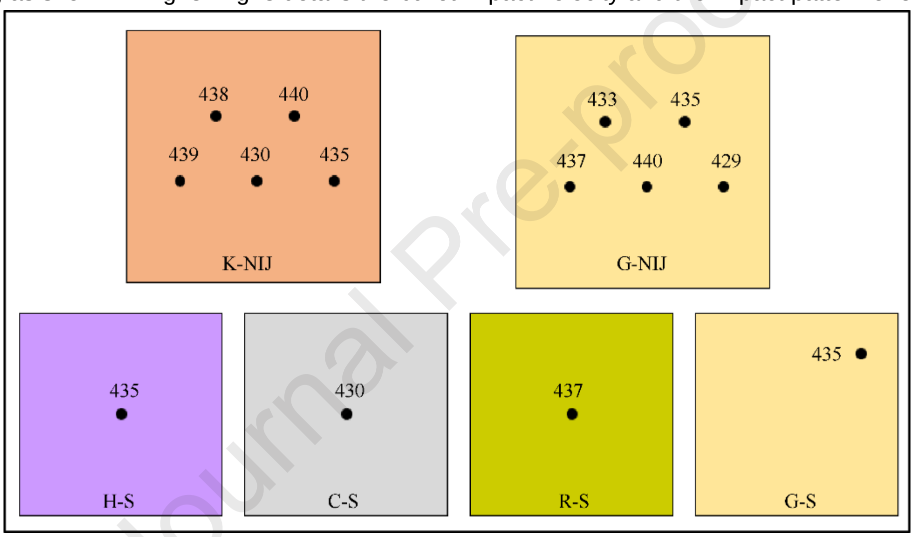

Fig. 3. Configuration and velocity of each bullet in the high-velocity impact test. K-NIJ and G-NIJ tested according to the NIJ test, whereas H-S, C-S, R-S were shot at the center, and G-S was shot at the side.

2.3. Computerized tomography (CT) scanning

Several nondestructive (NDT) methods were presented in the literature to characterize FRPs, such as pulse thermography (PT), high-frequency eddy current electromagnetic testing, ultrasonic testing, X-ray radiography, X-ray laminography, and high-resolution X-ray Computerized Tomography (CT) [33, 34]. These NDT methods exhibit significant differences in their underlying principles and application scopes. In this study, X-Ray Computerized Tomography was chosen because it utilizes X-rays and sophisticated computer algorithms to generate highly detailed cross-sectional images of the composite panels. By offering comprehensive visualizations of internal structures and properties, CT scanning offers invaluable insights to professionals, facilitating accurate analysis and evaluation of fiber-reinforced polymer matrix composites which constitutes the primary objective of this study. The aim is to obtain accurate and detailed images, enabling an in-depth investigation of the material's response to ballistic impacts and the behavior of the bullets upon interaction.

X-Ray Computerized Tomography was conducted for all panels after the ballistic testing using PHILIPS Ingenuity CT scanner at King Abdullah University Hospital (KAUH), as shown in Fig. 4. This advanced imagining technology allowed for a non-destructive, three-dimensional analysis of the tested panels, providing a comprehensive view of their internal structures to better understand the damage mechanisms that occurred during the ballistic examination and the condition of the bullets after impact. CT scans are essential for evaluating the condition of the panels and providing an overall analysis of the ballistic testing results.

Fig. 4. PHILIPS Ingenuity CT scanner for imaging ballistic composite panels, showing the alignment of the panel within the imaging equipment and the capability of 3D scanning from multiple angles.

2.4. Electromagnetic interference (EMI) shielding test

Representative specimens of the dimensions 3 cm×3 cm were tested from each panel to characterize their EMI shielding properties in the X-band frequency range (8–12 GHz). The Through-Reflect-Line (TRL) calibration method was performed prior to taking the measurements in accordance with the methodology described in Ref. [30]. A comprehensive set of transmission line measurements was performed to capture the scattering parameters (S_{11}, S_{21}), utilizing a vector network analyzer (VNA) Agilent E5071CENA connected to a Philips PM-7328-X-WR90 rectangular waveguide via coaxial cables as shown in Fig. 5. During the measurement process, the specimens were securely positioned between the two waveguide adapters to ensure accurate measurements.

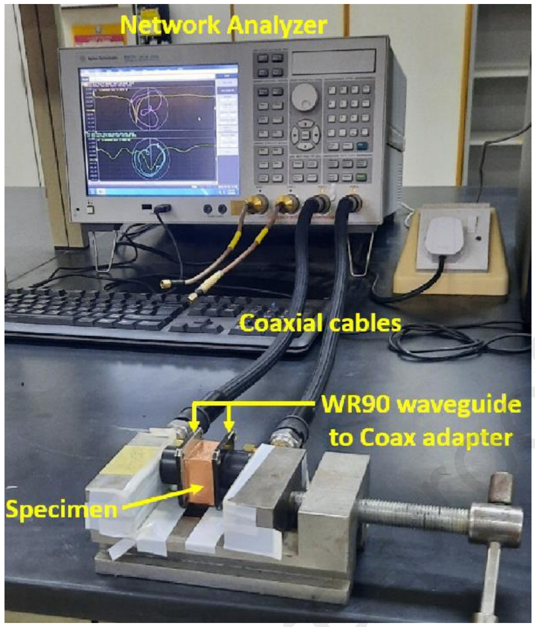

Fig. 5. Rectangular waveguide transmission line measurements setup.

3. Results and discussion

3.1. Ballistic test and CT scanning results

Figs. 6–11 provide comprehensive visual representations of both CT scan images and regular photos of the ballistic panels, which enhances the validity and reliability of the investigation. Fig. 6 shows CT scan images and photos of the tested Kevlar (K-NIJ) ballistic panel, demonstrating its ability to withstand high-velocity projectiles. The CT scan images and photos reveal that there was no penetration of the bullets through the panel or bullet fracture, indicating that the panel effectively stopped the five 9 mm bullets. However, a bulge in the back face of the panel was present, demonstrating the energy transfer that occurred during impact [5]. Furthermore, the representative through-the-thickness series of CT-scan images showed that there was a significant delamination and fiber tension in the middle layer of the panel, which subsequently propagated into a multilayer delamination that extended to all four edges of the panel [4, 35].

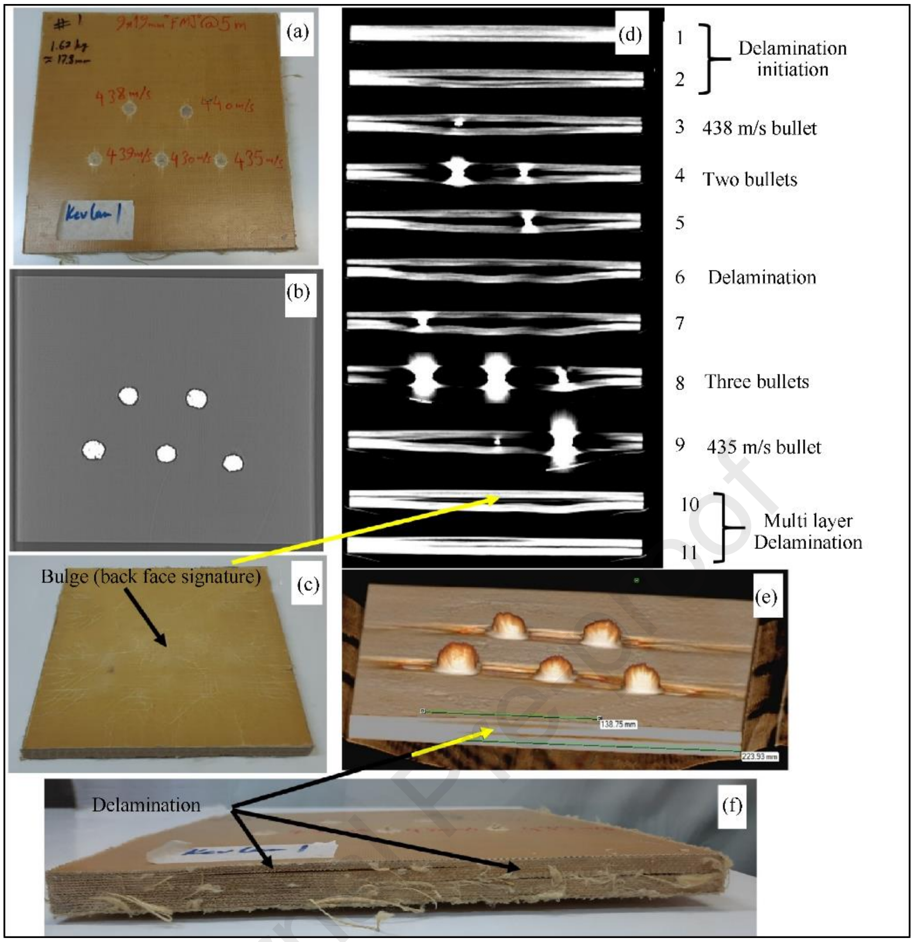

Fig. 6. CT scan images and photos of the tested Kevlar (K-NIJ) ballistic panel: (a) and (b) Front face-entry side; (c) Back face; (d) Series of representative CT scan images through the thickness; (e) 3D CT scan showing the edge delamination; (f) Edge delamination.

The CT scans and photos of the tested glass (G-NIJ) panel are presented in Fig. 7. The response of the fiber glass panel to high-velocity bullet strikes is different from that of Kevlar. The bullets did not penetrate the panel, instead, they fractured into fragments inside the panel. The bullets impact and fragmentation/shattering caused localized delamination within the composite panel, without leaving a visible bulge on the back face of the panel. However, the impact left a visible white discoloration on the back face of the panel, which is an indication of the internal delamination and internal damage to the matrix and fibers of the material. There is no visible delamination extending to the edges of the panel, and there is no indication of multilayer delamination. Rather, the delamination is confined and localized where the bullets fragmented. Overall, the CT scans and photos highlighted the unique response of the glass fiber panel to high-velocity projectiles compared to Kevlar. When a bullet strikes a composite panel, it generates a high amount of stress and pressure at the impact site. This stress and pressure cause the material to deform and absorb energy, as the bullet attempts to penetrate the panel. In the case of the Kevlar composite, the impact energy is converted into delamination inside the Kevlar cloth due to its high toughness and flexibility. This process causes the fibers to become densely packed together, preventing the striking bullet from further penetrating. However, with glass fiber composites, the impact energy and associated stresses lead to the fracture of the brittle glass fibers, resulting in localized damage within the material. As the bullet continues to penetrate the panel, the fractured fibers can cause the bullet to shatter further. The result suggests that the glass composite panel is capable of withstanding high-velocity impacts while maintaining its structural integrity, but may experience localized delamination under such conditions. In comparison, the Kevlar composite panel has the ability to endure high-velocity impacts but has a more profound effect on structural integrity.

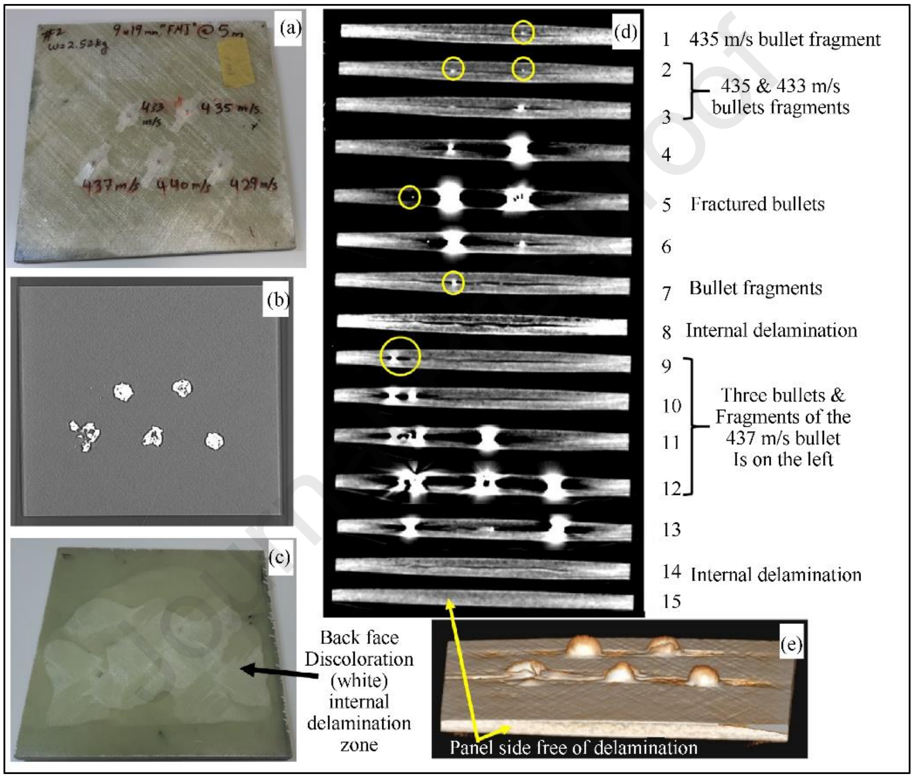

Fig. 7. CT scan images and photos of the tested Glass (G-NIJ) ballistic panel: (a) and (b): Front face-entry side; (c) Back face; (d) Series of representative CT scan images through the thickness; (e) 3D CT scan showing the free of delamination edge.

The high-velocity ammunition impact response of the Kevlar-Glass Hybrid (H-S) composite panel is presented in Fig. 8. The bullet did not penetrate the panel; instead, it stopped at the rear interfacial surface between the glass and Kevlar layers. This impact caused a partial fracture of the bullet, as evident by the bullet shrapnel at the representative through-the-thickness CT scan in Fig. 8(c). The rear interface between the glass and the Kevlar experienced a major delamination, which bulged on the back face of the panel. The CT scan presented in Fig. 8(d) reveals that the delamination zone, which appeared as a white color, did not extend to all four edges of the panel, as it was only apparent on one edge, which is depicted in Fig. 8(e). The result suggests that the Kevlar-Glass composite panel is capable of withstanding high-velocity ammunition impacts with a significant effect on its structural integrity at the interfaces.

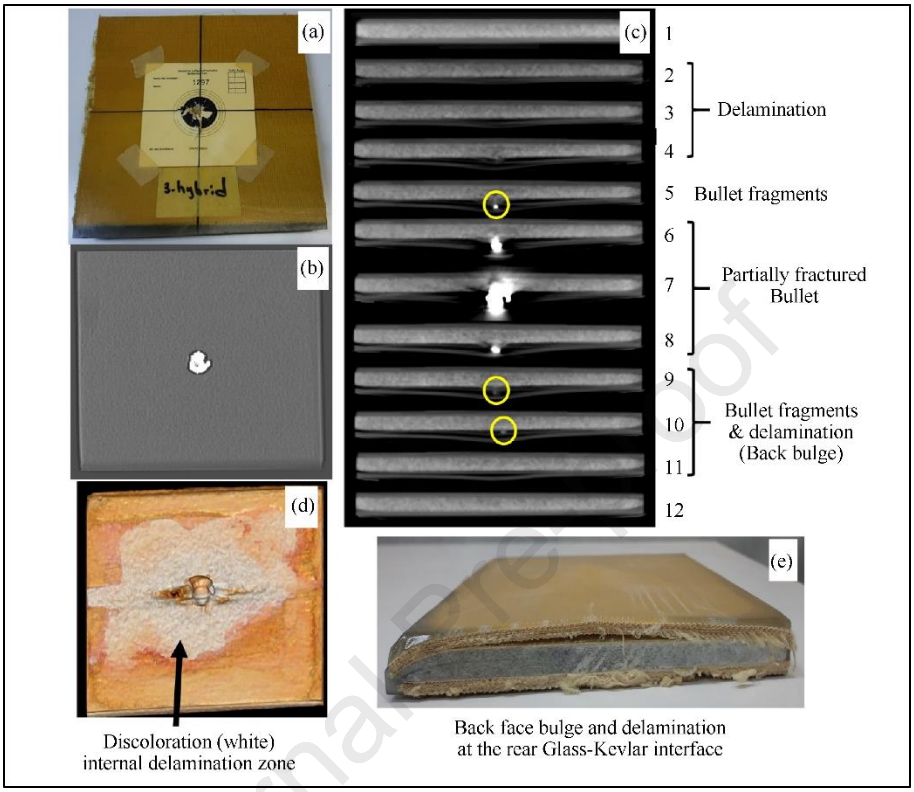

Fig. 8. CT scan images and photos of the tested Hybrid (H-S) ballistic panel: (a) and (b) Front face-entry side; (c) Series of representative CT scan images through the thickness; (d) 3D CT scan showing the internal delamination zone; (e) Bulge and Edge delamination

Fig. 9 exhibits the ballistic response of the glass fiber composite panel (G-S) struck with a bullet at its upper right side. The panel successfully prevented the bullet from penetrating, causing it to fracture and shatter inside. The impact resulted in localized delamination within the composite panel, which did not create a visible bulge on the back face of the panel, but instead a visible white discoloration appeared as an indication of the internal damage of the fibers and the matrix. The confined delamination on the upper right side of the panel extended to the nearby edge of the panel, as shown in Figs. 9(g) and 9(f), without any influence on the rest of the panel. No visible defects were observed in the entire panel except for the zone where the bullet struck. This implies the efficiency of this panel in resisting high-velocity ammunition without any effect on its structural integrity.

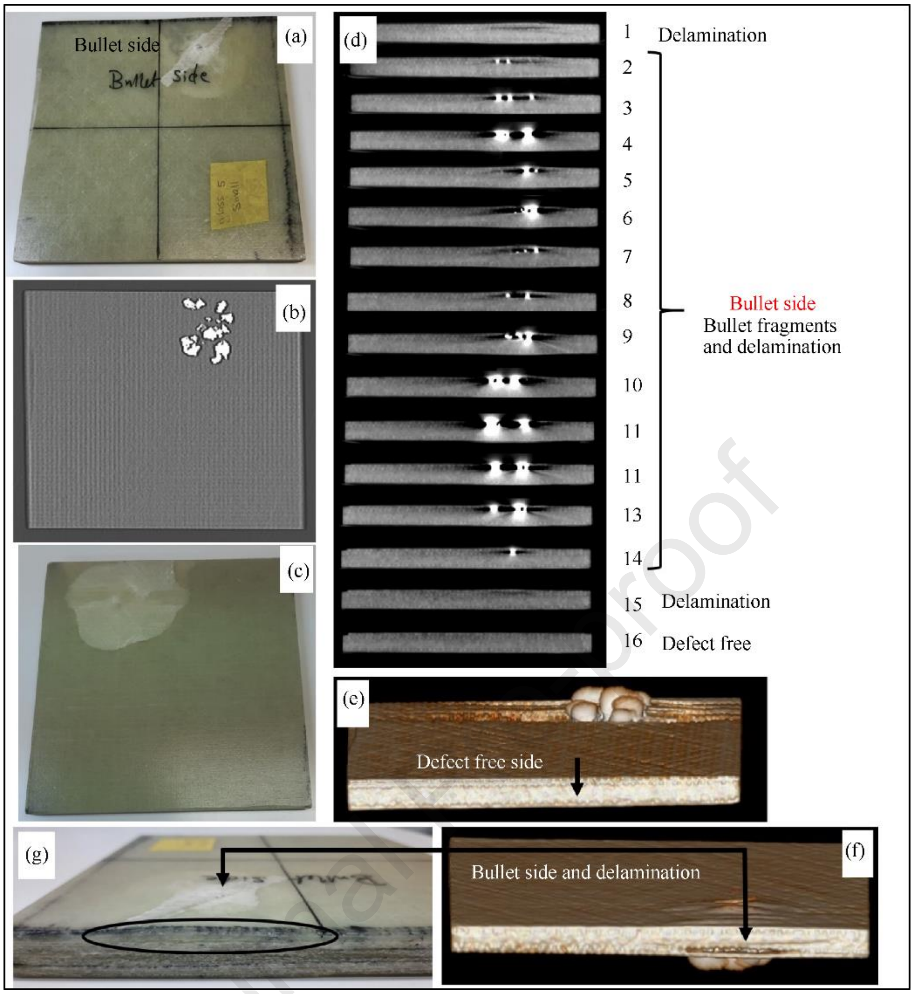

Fig. 9. CT scan images and photos of the tested Glass small (G-S) ballistic panel: (a) and (b) Front face-entry side; (c) Back face; (d) Series of representative CT scan images through the thickness; (e) 3D CT scan did not detect any defects; (f) and (g) Edge delamination.

Figs. 10 and 11 show the ballistic response of glass fiber-epoxy composite panels incorporating either SiC particles or crushed rubber (C-S and R-S, respectively). To make the panels lighter in weight, the number of glass fiber layers was decreased to 18. The layers that were removed were then substituted by either ceramic silicon carbide (SiC) particles or recycled crushed car tire rubber, as alternatives. The hope was to achieve the desired impact resistance by using damping elastic rubber or brittle ceramic particles while reducing the total weight. SiC particles were incorporated into the epoxy matrix with the objective of creating epoxy-ceramic rich layers that would function similarly to a flat ceramic plate in ceramic armors; to provide resistance against bullet penetration while maintaining a lighter weight. The panels were struck by a 9 mm bullet at the center, and both panels exhibited similar behavior to a large extent. Both panels exhibited ballistic penetration (perforation) with subsequent splintering, fiber breakage, and fiber pullout in the penetration path and on the back face. However, the distinguishing feature between the two panels was that a white discoloration was obvious in the back face of the R-S panel, whereas no white discoloration was observed in the C-S panel. Additionally, CT scan images revealed that the internal damage in the R-S panel was more severe compared to the C-S panel, and that the C-S panel was more capable of resisting the bullet, as small bullet fragments appeared inside the panel. These results suggest that incorporating SiC ceramic particles into the composite panel may be more effective in providing better ballistic resistance than using elastic rubber if the number or stacking sequence of the layers were modified. The panels′ structural integrity was intact despite the penetration.

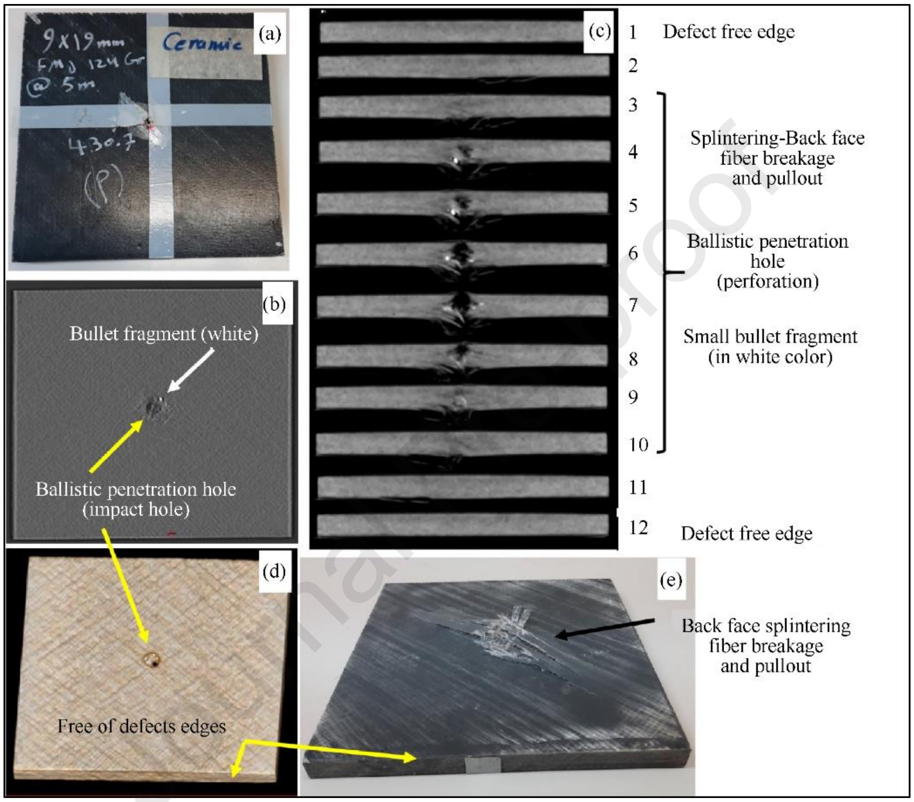

Fig. 10. CT scan images and photos of the tested SiC Ceramic (C-S) ballistic panel: (a), (b) and (d) Front face-entry side; (c) Series of representative CT scan images through the thickness; (e) Back face; (d) and (e) Free of delamination edge.

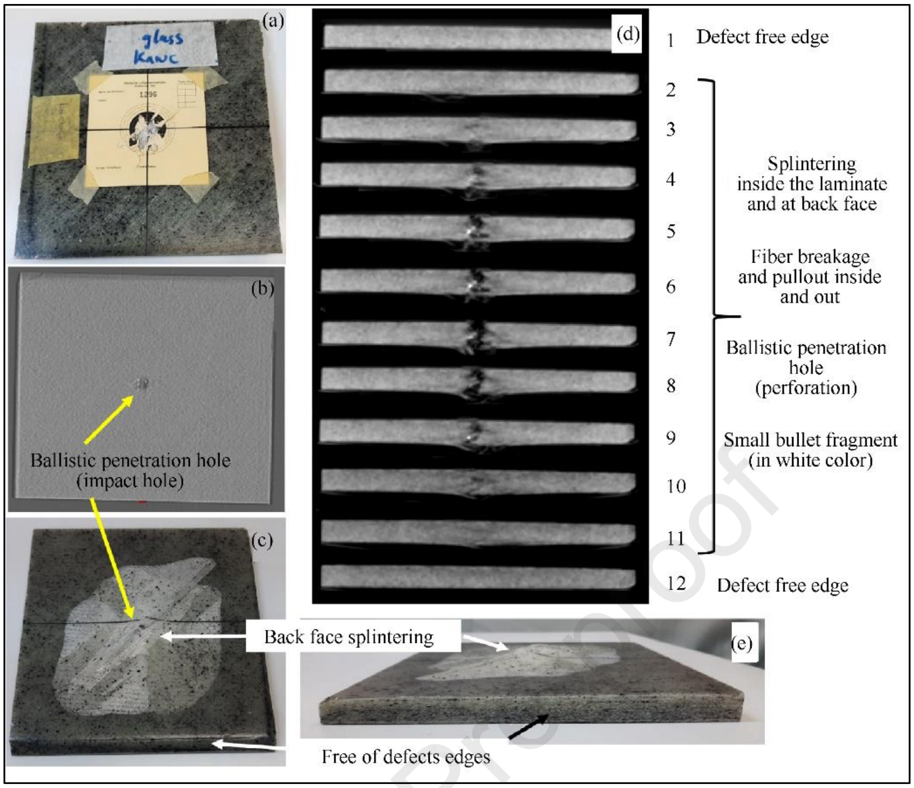

Fig. 11. CT scan images and photos of the tested rubber (R-S) ballistic panel: (a), (b) Front face-entry side; (c) Back face; (d) Series of representative CT scan images through the thickness; (e) free of delamination edge.

3.2 Electromagnetic interference shielding effectiveness of the ballistic laminates

The measured scattering parameters (S-parameters) obtained from the transmission line measurements were used to calculate several electromagnetic interference shielding parameters for each ballistic panel in the entire frequency range (8–12 GHz). These included the total EMI shielding effectiveness (SE), the reflectivity (*R*), the transmissivity (*T*), and the absorptivity (*A*), all of which were calculated using the corresponding Eqs. (1)–(4) [29, 36–39].

$$\text{EMI SE} = \text{SE} = 10\,\text{lg}\frac{1}{|S_{21}|^2} \quad (1)$$

$$R = \frac{P_R}{P_i} = |S_{11}|^2 = |S_{22}|^2 \quad (2)$$

$$T = \frac{P_T}{P_i} = |S_{21}|^2 \quad (3)$$

$$A = \frac{P_A}{P_i} = 1-(T+R) \quad (4)$$

where $|S_{ij}|^2$ is defined as the power ratio; $|S_{21}|^2$ parameter represents the ratio of the transmitted power through the shield to the incident power, while $|S_{11}|^2$ parameter represents the ratio of the reflected power from the shield to the incident power, P_R is the reflected power, P_A is the absorbed power, P_T is the transmitted power, and P_i is the incident power. Calculating the shielding parameters from a power balance perspective is an effective method to evaluate the shielding mechanisms.

Fig. 12 illustrates the EMI-SE of the ballistic composite panels within the X-band frequency range. It is clear that the EMI-SE curves for all ballistic panels follow a pattern similar to the normal distribution, where the peak SE value occurs at a particular frequency and subsequently declines across the remaining frequency range. The lowest achieved SE value was 6.2 dB at 12 GHz for the G-S panel, whereas the highest achieved SE value was 11.2 dB at 11 GHz for the K-NIJ panel. Across all panels, the EMI-SE remained almost constant in the 8-10.5 GHz range with slight variations, except for the G-NIJ and G-S panels. Interestingly, each panel exhibited a distinctive maximum SE value at a frequency that varied from the other panels. For example, K-NIJ demonstrated the highest achieved SE values of 11.2 dB at 11 GHz, whereas the G-NIJ panel exhibited the highest SE of 11 dB at 9.5 GHz. In addition, R-S and C-S displayed maximum SE value of 9.7 dB at 11 GHz and 10.5 GHz, respectively. The G-S panel revealed a peak SE of 10.5 dB at 10 GHz, while H-S showed a peak SE of 10.12 dB at 11 GHz.

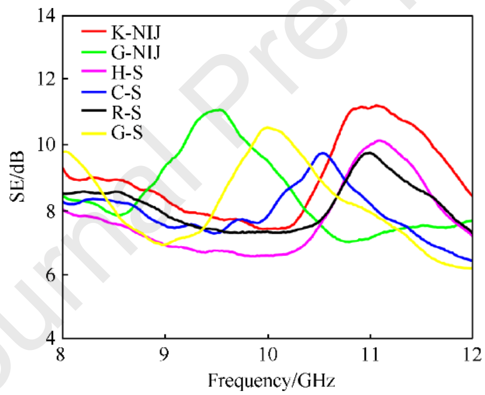

Fig. 12. EMI-SE of the ballistic composite panels.

The observed peaks in the shielding effectiveness curves are likely influenced by various factors, such as the specimen's thickness and constituents. These factors significantly impact the specimen′s properties, such as complex permittivity, complex permeability, loss tangent, and skin depth, all of which are influenced by the frequency [30, 40, [41]. Moreover, a relationship may be drawn between the specimen's thickness and the wavelength at which the peak appears [42]. The complexity of these peaks and their underlying mechanisms require a comprehensive analysis of these properties which falls beyond the scope of the current study and warrants further investigation in future studies.

The effectiveness of the composite panels in shielding against electromagnetic interference is determined by their absorptivity and reflectivity. Fig. 13 illustrates the absorptivity and reflectivity of the composite panels in the entire frequency range. The highest achieved absorptivity of 88% was observed for K-NIJ at 10.8 GHz, with a minimum of 60% at 8 GHz. Similarly, H-S showed an absorptivity of 87% at 11.1 GHz and a minimum of 60% at 8 GHz. This implies that 88% and 87% of the incident EM power is shielded by absorption, and only 12% of the incident power is transmitted through the composite panel at 8 GHz. A peak absorptivity of 80% was observed for the G-NIJ, G-S, C-S, and R-S panels at 9.4 GHz, 10 GHz, 10.6 GHz, and 11.2 GHz, respectively. Moreover, the lowest absorptivity observed on these panels ranged from 56% to 60% at 8 GHz, except for the glass panels G-NIJ and G-S, which showed a significantly smaller absorptivity of 48% and 42%. These findings highlight the variability in the electromagnetic shielding effectiveness of composite panels, with K-NIJ and H-S demonstrating the highest absorptivity. The highest reflectivity value of 44% was achieved for the glass panels, G-NIJ and G-S, at 8 GHz, whereas the other panels exhibited a reflectivity ranging from 10%-30% in the frequency range of 8-10.5 GHz indicating that absorption is the dominant mechanism of shielding, and that the composite panels are characterized as lossy materials [43−45]. Although the K-NIJ, H-S, R-S, and C-S composite panels differ in their shielding parameter values (SE, A, and R), they demonstrate a similar overall trend.

All panels exhibited a predominant absorption mechanism with absorptivity exceeding 50%, albeit with variations among different panels. The shielding mechanisms (absorptivity and reflectivity) are influenced by material properties, such as complex permittivity, loss tangent (loss factor), and skin depth (penetration depth). Relevant literature, including references [40, 41, 46, 47] indicate a direct relationship between complex permittivity, loss tangent, and skin depth with the frequency and the specimen′s constituents and thickness, thus influencing the shielding mechanisms of the materials. For instance, the loss tangent, which means the material's ability to dissipate EM wave energy through absorption, increases with increasing the specimen′s thickness in both glass and Kevlar composites [41]. The study also reveals that at 10 GHz, Kevlar exhibits a higher loss tangent than glass across various thicknesses. Additionally, the dielectric constant (real part of the complex permittivity) and dielectric loss (imaginary part of the complex permittivity) also influence the materials absorptivity vary with thickness and frequency for both materials [40]. The dielectric constant remains nearly identical for both Kevlar and glass composites regardless of frequency, while the penetration depth and the dielectric loss varies with frequency for both materials. Due to the intricacy of the analysis, to fully comprehend and interpret the reasons behind the shielding mechanisms, a complete analysis of the properties of the materials are required in future studies.

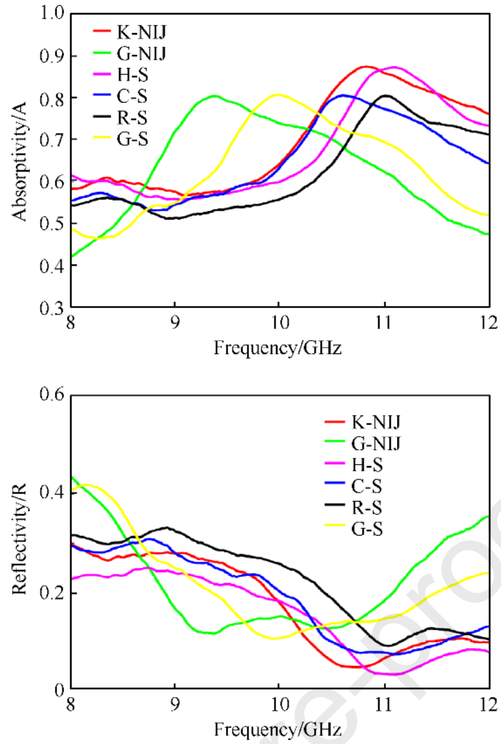

Fig. 13. Reflectivity (R) and Absorptivity (A) of the ballistic composite panels.

These findings provide valuable insights into the EMI shielding properties of various ballistic composite panels and their potential suitability for use in applications that require effective protection against electromagnetic interference. Moreover, the results suggest that the choice of composite panel type may significantly impact the shielding effectiveness at different frequencies, highlighting the importance of carefully selecting the appropriate composite material for a given application based on the frequency range.

4. Conclusions

This study aims to address several critical points related to the investigation of ballistic and electromagnetic interference shielding properties in composites made of Kevlar and glass. While the ballistic properties of composites are commonly studied for materials like Kevlar and carbon, glass composites have received relatively less attention in this area. Similarly, EMI shielding characteristics are often explored in composites made of carbon due to their high electrical conductivity, while investigations involving Kevlar or glass composites are limited due to their lower electrical conductivities. In this study, shield materials made of Kevlar and glass composites that provide effective protection against high-velocity ballistic impact and electromagnetic interference shielding via absorption were developed. Six fiber-reinforced epoxy composite panels with different fabric materials and stacking sequences were fabricated using a hand-layup vacuum bagging process. The panels consisted of Kevlar and glass fibers at varying orientations and were combined with fillers during the fabrication process. Two panels were tested using the National Institute of Justice ballistic resistance protective materials test, NIJ 0108.01 Standard- Level IIIA (9 mm×19 mm FMJ 124 g). One panel consisted of 15 layers of Kevlar (K-NIJ) and another of 26 layers of multidirectional glass fiber (G-NIJ). Four additional panels were tested: one comprised of a hybrid structure consisting of 20 layers of Kevlar and glass, where the glass was sandwiched between two Kevlar faces (H-S); one made of 20 layers of multidirectional glass with silicone carbide ceramic particles (C-S); one made of 20 layers of multidirectional glass with recycled rubber in the epoxy matrix (R-S); and one made of 24 layers of multidirectional glass (C-S). Of these, three panels (H-S, C-S, and R-S) were fired at the center, while the G-S panel was fired at the edge with a 9 mm bullet at an average muzzle velocity of 434 m/s. EMI shielding measurements in the X-band frequency range via the reflection-transmission method were conducted for representative samples of all panels.

The results indicated that four panels, namely K-NIJ, G-NIJ, H-S, and G-S, are capable of withstanding high-velocity impact and preventing the bullet from penetrating through the panels while maintaining their structural integrity in contrary to previous research studies which reported full penetration or partial damage of the ballistic panels [48, 49]. However, localized delamination with variable severity may occur under such conditions. The panels made of glass fiber showed no signs of bulging or delamination that extended to the panel edges, while the Kevlar panels exhibited delamination that extended to the panel edges. The panels which consisted of 20 layers of glass with SiC and rubber filler, exhibited ballistic penetration with subsequent splintering and fiber breakage on the back face. The EMI measurements indicated that all panels functioned as a lossy medium and relied primarily on absorption as the dominant shielding mechanism. However, each panel exhibited peak absorptivity at different frequencies. K-NIJ and H-S panels demonstrated the highest absorptivity of 88%, whereas the remaining panels exhibited a peak absorptivity of 80%. The low-cost glass fiber composite materials developed using a well-known and simple manufacturing method exhibited remarkable ballistic protection and effective EMI shielding absorption, making them materials with great potential for diverse applications. It is noteworthy that EMI shielding properties are increasingly crucial in the aerospace and aviation sectors both military and commercial, particularly in the context of modern "fly-by-wire" systems and other electronic components found in aircraft and aerospace applications. The need for materials that effectively protect these electronics from EM signal interference and impact damage, such as the protection of black boxes, underscores the significance of this study's findings. It is important to note that EMI shields are not limited to these applications alone; they are also essential in medical equipment to reduce electromagnetic pollution.

It is essential to acknowledge that the current study represents the initial stage of a broader, long-term project. The subsequent stage of the project will be dedicated to further research aimed at reducing the weight of these composites. By addressing weight reduction, the study aims to enhance the overall performance and applicability of these materials in various practical scenarios.

Acknowledgments

This work was financially supported by the Deanship of Research – Jordan University of Science and Technology, Irbid – Jordan. Grant number 318/2021. Author is grateful to The Test and Evaluation Department at Jordan Design and Development Bureau (JODDB) for conducting the NIJ tests. Also, author is deeply thankful to the department of radiology staff, especially Mr. Bashar M. Al-Shorman, at King Abdullah University Hospital (KAUH) for conducting the CT scan.

Author contribution

This study was conducted by the sole author (XXX) who designed the experiment, manufactured the panel, participated in conducting the NIJ tests, and conducted the EMI shielding measurements and the participated in conducting the CT-Scans in the hospital. She is the sole author who wrote the manuscript.

Supplementary information

Additional supplementary information pertaining to the methods, results, and/or analysis of the study is available upon request from the author.

Ethical approval

Author confirms that no experiments involving human subjects were conducted. Therefore, the study does not raise any ethical concerns related to the protection of humans.

References

[1] S. Wu, P. Sikdar, and G. S. Bhat, "Recent progress in developing ballistic and anti-impact materials: Nanotechnology and main approaches," *Def. Technol.*, 2022, doi: 10.1016/j.dt.2022.06.007.

[2] M. Alubel, F. Boussu, and P. Bruniaux, "Dynamic impact protective body armour : A comprehensive appraisal on panel engineering design and its prospective materials," *Def. Technol.*, vol.17, pp. 2027-2049, 2021, doi: 10.1016/j.dt.2021.03.016.

[3] I. G. Crouch, "Body armour – new materials, new systems," *Def. Technol.*, vol.15, pp. 241-253, 2019, doi: 10.1016/j.dt.2019.02.002.

[4] L. Ding, X. Gu, P. Shen, and X. Kong, "Ballistic Limit of UHMWPE Composite Armor under Impact of of Ogive-nose projectile," *Polymers.*, vol. 14, art. no. 4866, 2022.

[5] M. A. Abtew, F. Boussu, P. Bruniaux, C. Loghin, and I. Cristian, "Ballistic impact mechanisms – A review on textiles and fibre-reinforced composites impact responses," *Compos. Struct.*, vol. 223, art.no 110966, 2019, doi: 10.1016/j.compstruct.2019.110966.

[6] A. Bhatnagar, "Lightweight Ballistic Composites : Military and Law-Enforcement Applications," 2nd edition, Woodhead publishing series in composites science and engineering, pp. 3–4, 2016.

[7] M. A. Abtew, F. Boussu, P. Bruniaux, and Y. Hong, "Dynamic Impact Surface Damage Analysis of 3D Woven Para-Aramid Armour Panels Using NDI Technique," Polymers, vol.13, pp. 1–21, 2021.

[8] Y. S. Lee, E. D. Wetzel, and N. J. Wagner, "The ballistic impact characteristics of Kevlar woven fabrics impregnated with a colloidal shear thickening fluid," *J. Mater.Sci*, vol. 8, pp. 2825–2833, 2003.

[9] D. Ma, A. Manes, S. C. Amico, and M. Giglio, "Ballistic strain-rate-dependent material modelling of glass-fibre woven composite based on the prediction of a meso-heterogeneous approach," *Compos. Struct.*, vol. 216, pp. 187–200, 2019, doi: 10.1016/j.compstruct.2019.02.102.

[10] J.C. Farias-Aguilar, M.J. Ramı´rez-Moreno, D.M. Gonzalez-Garcı´a, L. Tellez-Jurado, H. Balmori-Ramı´rez, "Evaluation of the ballistic protection level of (glass- fiber reinforced polyamide 6) -aramid fabric sandwich composite panels,"*JMR&T*, vol.12, pp.1606-1614, 2021, doi: 10.1016/j.jmrt.2021.03.088.

[11] N. Domun *et al.*, "Ballistic impact behaviour of glass fibre reinforced polymer composite with 1D/2D nanomodified epoxy matrices," *Compos. Part B*, vol. 167, pp. 497–506, 2019, doi: 10.1016/j.compositesb.2019.03.024.

[12] M. Grujicic., G.Arakere, T. He, W.C. Bell, B.A. Cheeseman, C.F. Yen, B.Scott, "A ballistic material model for cross-plied unidirectional ultra-high molecular-weight polyethylene fiber-reinforced armor-grade composites," *Mater. Sci. Eng. A*, vol. 498, no. 1–2, pp. 231–241, 2008, doi: 10.1016/j.msea.2008.07.056.

[13] H. Wang, D. Weerasinghe, P. J. Hazell, D. Mohotti, E. V. Morozov, and J. P. Escobedo-Diaz, "Ballistic impact response of flexible and rigid UHMWPE textile composites: Experiments and simulations," *Def. Technol.*, 2022, doi: 10.1016/j.dt.2022.08.009.

[14] R. Stopforth and S. Adali, "Experimental study of bullet-proofing capabilities of Kevlar, of different weights and number of layers, with 9 mm projectiles," *Def. Technol.*, vol. 15, no. 2, pp. 186–192, 2019, doi: 10.1016/j.dt.2018.08.006.

[15] F. D. C. Garcia Filho, M. S. Oliveira, A. C. Pereira, L. F. C. Nascimento, J. Ricardo Gomes Matheus, and S. N. Monteiro, "Ballistic behavior of epoxy matrix composites reinforced with piassava fiber against high energy ammunition," *J. Mater. Res. Technol.*, vol. 9, no. 2, pp. 1734–1741, 2020, doi: 10.1016/j.jmrt.2019.12.004.

[16] K. J. Narayana and R. Gupta Burela, "A review of recent research on multifunctional composite materials and structures with their applications," *Mater. Today Proc.*, vol. 5, no. 2, pp. 5580–5590, 2018, doi: 10.1016/j.matpr.2017.12.149.

[17] C. González, J. J. Vilatela, J. M. Molina-Aldareguía, C. S. Lopes, and J. LLorca, "Structural composites for multifunctional applications: Current challenges and future trends," *Prog. Mater. Sci.*, vol. 89, no. April 2017, pp. 194–251, 2017, doi: 10.1016/j.pmatsci.2017.04.005.

[18] W. Wu, W. Hu, G. Qian, H. Liao, X. Xu, and F. Berto, "Mechanical design and multifunctional applications of chiral mechanical metamaterials: A review," *Mater. Des.*, vol. 180, art.no. 107950, 2019, doi: 10.1016/j.matdes.2019.107950.

[19] C. J. Von Klemperer and D. Maharaj, "Composite electromagnetic interference shielding materials for aerospace applications," *Compos. Struct.*, vol. 91, no. 4, pp. 467–472, 2009, doi: 10.1016/j.compstruct.2009.04.013.

[20] M. Wachowski, R. Kosturek, V. Hutsaylyuk, and L. Sniezek, " Lightweight multi-layer material for military applications with enhanced ballistic properties and ability for electromagentic interference (EMI) shielding," 1st international symposium in electronic engineering, information technology, and education, 2019.

[21] S. Verma, M. Dhangar, S. Paul, K. Chaturvedi, and M. Akram, "Recent Advances for Fabricating Smart Electromagnetic Interference Shielding Textile: A Comprehensive Review," *Electron. Mater. Lett.*, no. 0123456789, 2022, doi: 10.1007/s13391-022-00344-w.

[22] E. Mikinka, M. Siwak, "Recent advances in electromagnetic interference shielding properties of carbon-fibre-reinforced polymer composites – a topical review," *J Mater Sci*: *Mater Electron,* vol. 32, no. 20. pp. 24585–24643, 2021, doi: 10.1007/s10854-021-06900-8

[23] H. Zhang, J. Li, Y. Pan, Y. Liu, and N. Mahmood, "Flexible carbon fiber-based composites for electromagnetic interference shielding," *Rare Met.*, vol. 41, no. 11, pp. 3612–3629, 2022, doi: 10.1007/s12598-022-02057-3.

[24] P. Banerjee and Y. Bhattacharjee, "Lightweight Epoxy-Based Composites for EMI Shielding Applications," vol. 49, no. 3, pp. 1702–1720, 2020, doi: 10.1007/s11664-019-07687-5.

[25] Y. Zhang, T. Pan, and Z. Yang, "Flexible polyethylene terephthalate / polyaniline composite paper with bending durability and effective electromagnetic shielding performance," *Chem. Eng. J.*, vol. 389, 2019, art. no. 124433, 2020, doi: 10.1016/j.cej.2020.124433.

[26] Y. Zhang, M. Qiu, Y. Yu, B. Wen, and L. Cheng, "A Novel Polyaniline-Coated Bagasse Fiber Composite with Core – Shell Heterostructure Provides Effective Electromagnetic Shielding Performance," ACS Appl Mater Interfaces., vol. 9, pp. 809-818, 2017, doi: 10.1021/acsami.6b11989.

[27] P. Verma, P. Saini, R. S. Malik, and V. Choudhary, "Excellent electromagnetic interference shielding and mechanical properties of high loading carbon-nanotubes/polymer composites designed using melt recirculation equipped twin-screw extruder," *Carbon N. Y.*, vol. 89, pp. 308–317, 2015, doi: 10.1016/j.carbon.2015.03.063.

[28] G. Verma and K. P. Ray, "Design , Fabrication and Characteristics of Eco- Friendly Microwave Absorbing Materials : A Review Design , Fabrication and Characteristics of Eco-Friendly Microwave Absorbing Materials : A Review," *IETE Tech. Rev.*, vol. 39, no. 4, pp. 1–19, 2021, doi: 10.1080/02564602.2021.1927865.

[29] N. Abdelal, "Electromagnetic interference shielding of stitched carbon fiber composites," *J. Indus.Tex*, vol. 49, no. 6, pp. 773–790, 2018, doi: 10.1177/1528083718798632.

[30] N. Abdelal, N. Dib, D. Young, and A. Slanker, "Electromagnetic interference shielding and dielectric properties of graphene nanoplatelets / epoxy composites in the x-band frequency range," *J. Mater. Sci.*, vol. 57, no. 29, pp. 13928–13944, 2022, doi: 10.1007/s10853-022-07475-3.

[31] N. Abdelal, A. Alomari, and N. Dib, "Armadillo shell-inspired carbon nanotubes-epoxy composites developed using 3D printing for electromagnetic interference shielding," *Addit. Manuf.*, vol. 71, no. May, p. 103599, 2023, doi: 10.1016/j.addma.2023.103599.

[32] D. Micheli, A.Vricella, R. Pastore, A. Delfini, A. Giusti, M. Albano,M. Marchetti, F. Moglie, V. M. Primiani, "Ballistic and electromagnetic shielding behaviour of multifunctional Kevlar fiber reinforced epoxy composites modified by carbon nanotubes," *Carbon N. Y.*, vol. 104, pp. 141–156, 2016, doi: 10.1016/j.carbon.2016.03.059.

[33] I. Hakim, D. Schumacher, V. Sundar, S. Donaldson, A. Creuz, R. Schneider, J. Keller, C. Browning, D. May, M. Abo Ras, N. Meyendorf. "Volume Imaging NDE and Serial Sectioning of Carbon Fiber Composites," *AIP Conference Proceedings,* vol. 37, 2018, doi: 10.1063/1.5031590.

[34] D. Schumacher, N. Meyendorf, I. Hakim, U. Ewert., "manufacturing process Defect Recognition in CFRP Components Using Various NDT Methods within a Smart Manufacturing Process," *AIP Conference Proceedings,* vol. 020024, 2018, doi: 10.1063/1.5031521.

[35] R. Chricker, S. Mustacchi, E. Massarwa, R. Eliasi, J. Aboudi, and R. H. Ali, "Ballistic Penetration Analysis of Soft Laminated Composites Using Sublaminate Mesoscale" Modeling, *Comp. Sci.,* vol.5, art.no. 21, 2021.

[36] D. D. L. Chung, "Materials for electromagnetic interference shielding," *Mater. Chem. Phys.*, vol. 255, no. art.no. 123587, 2020, doi: 10.1016/j.matchemphys.2020.123587.

[37] D. Munalli, G. Dimitrakis, D. Chronopoulos, S. Greedy, and A. Long, "Electromagnetic shielding effectiveness of carbon fibre reinforced composites," *Compos. Part B Eng.*, vol. 173, pp. 1–28, 2019.

[38] H. Gao, C. Wang, Z. Yang, and Y. Zhang, "3D porous nickel metal foam / polyaniline heterostructure with excellent electromagnetic interference shielding capability and superior absorption based on pre-constructed macroscopic conductive framework," *Compos. Sci. Technol.*, vol. 213, no. June, p. 108896, 2021, doi: 10.1016/j.compscitech.2021.108896.

[39] C. Wang, H. Gao, D. Liang, S. Liu, H. Zhang. H. Guan, Y. Wu, Y. Zhang., "Effective fabrication of flexible nickel chains / acrylate composite pressure - sensitive adhesives with layered structure for tunable electromagnetic interference shielding," *Adv. Compos. Hybrid Mater.*, pp. 2906–2920, 2022, doi: 10.1007/s42114-022-00482-7.

[40] R. Zoughi and B. Zonnefeld, "Permittivity Characteristics of Kevlar, Carbon Composites, E-Glass, and Rubber (33% Carbon) at X-Band (8-12 GHZ)," *Review of Progress in Quantitative Nondestructive Evaluation*, vol. 10B, pp. 1431–1436, 1991.

[41] A.S. Abu Bakar, M. I. Misnon, D. K. Ghodgaonkar, N. Khadril, J.H. Salleh, W.Y. W.Ahmad, M. Dahalan, M. Ramli., "Microwave Nondestructive Evaluation of Textile Composites for Comparison Between Electrical and Physical Properties Microwave Nondestructive Evaluation of Textile Composites for Comparison Between Electrical and Physical Properties," 28th General Assembly of the International Union of Radio Science (URSI), New Delhi, India, 2005.

[42] F. Costa, "Electromagnetic Characterisation of Materials by Using Transmission / Reflection (T / R) Devices," 2017, doi: 10.3390/electronics6040095.

[43] N. C. Das, D. Khastgir, T. K. Chaki, and A. Chakraborty, "Electromagnetic interference shielding effectiveness of carbon black and carbon fibre filled EVA and NR based composites," *Compos. Part A*, vol. 31, pp. 1069–1081, 2000.

[44] A. Fida, M. J. Mughal, and D. E. Anagnostou, "C-Band and X-Band Switchable Frequency-Selective Surface," *Electronics*, vol. 10, pp. 1–15, 2021.

[45] A. Uddin, D. Estevez, Y. Luo, and H. Peng, "Lightweight microwire / graphene / silicone rubber composites for efficient electromagnetic interference shielding and low microwave reflectivity Lightweight microwire / graphene / silicone rubber composites for efficient electromagnetic interference shielding and low microwave reflectivity," *Comp. Sci. Tech*, vol.189, art.no. 108022, 2020, doi: 10.1016/j.compscitech.2020.108022.

[46] Z. Li, J. Ma, H. Ma, and X. Xu, "Properties and Applications of Basalt Fiber and Its Composites," 2018 IOP Conf. Ser.: Earth Environ. Sci. 186 012052, doi 10.1088/1755-1315/186/2/012052.

[47] B. Golchinfar, M. Rutner, and D. Donskoy, "Computational and Experimental Testing of Thermo-Chemical Structural Health Monitoring of Composites," ASCE EMIPMC 2016 conference - Vanderbilt University, Nashville, USA, 2016.

[48] M. Ansari and A. Chakrabarti, "Ballistic performance of unidirectional glass fiber laminated composite plate under normal and oblique impact," *Procedia Eng.*, vol. 173, pp. 161–168, 2017, doi: 10.1016/j.proeng.2016.12.053.

[49] M. Ansari and A. Chakrabarti, "Influence of projectile nose shape and incidence angle on the ballistic perforation of laminated glass fi ber composite plate," *Compos. Sci. Technol.*, vol. 142, pp. 107–116, 2017, doi: 10.1016/j.compscitech.2016.12.033.

Highlights

- Development of cost-effective shield composite materials combining high-velocity ballistic impact protection and electromagnetic interference (EMI) shielding via absorption.
- Fabrication and testing of six fiber-reinforced epoxy composite panels with different fabric materials and stacking sequences.
- Panels (K-NIJ, G-NIJ, H-S, and G-S) successfully withstand high-velocity impact, stopping bullet penetration while maintaining structural integrity.
- EMI measurements show absorptivity above 65% for all panels, with K-NIJ and H-S demonstrating the highest absorptivity.
- Novel, cost-effective, multifunctional glass fiber epoxy composite developed with superior ballistic protection compared to Kevlar.
- Demonstrates high EMI shielding absorption and shows promise for military and defense applications.

Declaration of interests

☒ The authors declare that they have no known competing financial interests or personal relationships that could have appeared to influence the work reported in this paper.

☐The authors declare the following financial interests/personal relationships which may be considered as potential competing interests: